

Structural and optical study of indium and gallium arsenide nanostructures prepared by magnetron sputtering

S. Torres- Jaramillo¹, C. Pulzara-Mora¹, R. Bernal-Correa^{2,*}, M. Venegas de la Cerda³,
S. Gallardo-Hernández³, M. López-López³, A. Pulzara-Mora¹

Edited by

Juan Carlos Salcedo-Reyes
(salcedo.juan@javeriana.edu.co)

1. Universidad Nacional de Colombia, sede Manizales, Facultad de Ciencias Exactas y Naturales, Departamento de Física y Química, Laboratorio Nanoestructuras Semiconductoras, Campus la Nubia, Manizales, Colombia.

2. Universidad Nacional de Colombia, sede Orinoquia, Unidad de Docencia y Formación, km 9 vía Arauca - Caño Limón, Arauca Colombia.

3. Centro de Investigación y Estudios Avanzados CINVESTAV-IPN, Departamento de Física, México D.F, México.

* rabernalco@unal.edu.co

Received: 14-08-2018

Accepted: 04-07-2019

Published on line: 19-11-2019

Citation: Torres-Jaramillo S, Pulzara-Mora C, Bernal-Correa R, Venegas de la Cerda M, Gallardo-Hernández S, López-López M, Pulzara-Mora A. Structural and optical study of indium and gallium arsenide nanostructures prepared by magnetron sputtering, *Universitas Scientiarum*, 24 (3): 523-542, 2019. doi: 10.11144/Javeriana.SC24-3.saos

Funding:

Grants 38416 and 28096 by the Research Department of Universidad Nacional de Colombia, Manizales-DIMA and with the Francisco José de Caldas Scholarship (No. 528) awarded by COLCIENCIAS.

Electronic supplementary material: N.A.



Abstract

Currently, the obtention of nano-structures based on III-V materials is expensive. This calls for novel and inexpensive nanostructure manufacturing approaches. In this work we report on the manufacture of a nanostructures consisting of alternating layers of In and GaAs on a Si substrate by magnetron sputtering. Furthermore, we characterized the produced nanostructures using secondary ion mass spectroscopy (SIMS), X-ray diffraction analysis, and Raman spectroscopy. SIMS revealed variation in the concentration of In atoms across In/GaAs/In interphases, and X-ray diffraction revealed planes corresponding to phases associated with GaAs and InAs due to In interfacial diffusion across GaAs layers. Finally, in order to study the composition and cristal quality of the manufactures nanostaructures, Raman spectra were taken using laser excitation lines of 452 nm, 532 nm, and 562 nm at different points across the nanostructures. This allowed to determine the transverse and longitudinal optical modes of GaAs and InAs, characteristic of a two-mode behavior. An acoustic longitudinal vibrational mode LA(Γ) of GaAs and an acoustic longitudinal mode activated by disorder (DALA) were observed. These resulted from the substitution of Ga atoms for In atoms in high concentrations due to the generation of Ga(VGa) and/or As(VAs) vacancies. This set of analyses show that magnetron sputtering can be a viable and relatively low-cost technique to obtain this type of semiconductors.

Keywords: III-V semiconductors; Raman spectroscopy; SIMS; X-ray.

Introduction

The development of III-V nanostructure layers by epitaxial growth technologies has prompted the production of materials with functional properties suitable to develop optoelectronic devices [1-8] and more efficient solar cells than those traditionally manufactured with semiconductors such as germanium (Ge) and silicon (Si) [9-12]. Currently, the preparation of these nanostructures is costly, so less expensive preparation methods,

such as magnetron sputtering, are being explored. The aim of these nanostructure preparation alternatives is to obtain good structural quality III-V semiconductors compatible with traditional semiconductor technology [13-16]. The success of these efforts will translate in the production of low-cost optical devices, compared with some widely used epitaxial techniques, such as molecular-beam epitaxy (MBE) [17-23].

Among the III-V semiconductors alloys containing elements such as gallium (GS), arsenic (As), indium (In), among others, are of interest because the controlled introduction of impurities in the semiconductor matrix generates stoichiometry-dependent changes that vary its optical and electrical properties. For instance, gallium arsenate (GaAs) doped with indium (leading to InGaAs) has the possibility of obtaining bandgaps from 0.36 eV (corresponding to InAs) up to 1.44 eV (corresponding to GaAs) [24, 25]. InGaAs has been synthesized using physical and chemical methods such as metal-organic chemical vapor deposition (MOCVD) and/or molecular-beam epitaxy [26, 27], in which complex procedures and special experimental conditions are required [28, 29]. Another functional technique for the preparation of this type of alloys is magnetic field-assisted cathodic sputtering, known as or magnetron sputtering. With this technique semiconductor layers can be deposited on monocrystalline, polycrystalline, and/or amorphous substrates. However, reports on the use of this technique for the growth of polycrystalline III-V semiconductors are scarce [30, 31].

In this paper, the results of the manufacture of alternating layers of indium and GaAs on a silicon substrate (100) by magnetron sputtering, and their characterization by secondary ion mass spectroscopy (SIMS), X-ray diffraction, and Raman spectroscopy are reported. SIMS is a surface material characterization technique, capable of detecting surface impurities in concentrations below one part per million and in bulk (of the order of one part per billion), with excellent depth resolution (~ 10 nm). SIMS also has the capacity to directly provide composition vs. depth profiles in real space, making this approach appropriate to characterize thin films, multilayers, and heterostructures, such as those of the present work [32]. To study InGaAs ternary formation by indium interfacial diffusion in GaAs layers, several composition spectra were obtained at given points across the structure. Finally, the structural characterization was performed by means of X-rays and Raman spectroscopy using three excitation lines.

Material and methods

High-purity (95.5 %) indium and GaAs targets (100) were used to obtain the samples. The employed silicon substrates (100) were first degreased with acetone and methanol. Next, they were cleaned with 2 % hydrofluoric

acid, rinsed with deionized water, dried with nitrogen, and introduced into the magnetron sputtering chamber. Then, the intended nanostructure was constructed as follows: firstly, a GaAs layer was deposited, operating the GaAs target for 30 minutes. Subsequently, the GaAs-associated shutter was closed, and the substrate's temperature was lowered to 300 °C. Upon reaching this temperature, the indium target source was turned on for a given time ($t_d = 5, 10$ and 15 minutes for each of the samples of interest, M1-M3). This process was repeated opening and closing the shutters, one at a time, until three GaAs/In/GaAs/In/GaAs nanostructures were formed. The shutters of the two targets do not completely close the targets, allowing indium atoms and GaAs molecules to escape. The employed experimental conditions are shown in **Table 1**.

Secondary ion mass spectroscopy measurements were performed in a TOF-SIMS-5 reflection analyzer (ION-TOF, Germany) consisting of a 5 keV primary energy beam with an approximate angle of 45 ° with respect to the sample and a double-focusing mass spectrometer equipped with a photomultiplier. X-ray diffraction measurements were made in a Rigaku miniflex equipment (Rigaku, Japan) in a range of $20^\circ \leq 2\theta \leq 60^\circ$. Raman spectra were taken with a N8 NEOS SENTERRA Bruker equipment (Bruker, USA) that combines a SENTERRA Raman spectrometer with a Nano's N8 NEOS atomic force microscope.

Results and Discussion

Secondary ion mass spectroscopy

The constructed Indium-GaAs interfaces (samples M1-M3) were analyzed by determining the distribution of indium and GaAs in the layers by concentration-depth spectra with secondary ion mass spectroscopy (SIMS). This made it possible to accurately infer the shape of indium/GaAs structures [33]. Component concentrations, as functions of the thickness in the M1 sample, are shown in **Fig. 1a**. The signal's amplitude was normalized to the unit to identify the relative contrast of the ions throughout the sample. The curves corresponding to gallium and arsenic showed periodic modulation and revealed layer formation with not very well-defined interfaces in the M1 sample. In this spectrum, a less significant change in the intensity of indium was observed; this was due to indium diffusion in the GaAs layers. In the case of the M2 and M3 samples, a similar behavior is observed in which the amplitude of the oscillations specific to each structure changed. This was due to the variation in the preparation times (and/or thickness) of the samples.

Indium diffusion in the SIMS depth profiles is in accordance with X-ray diffraction (addressed in the following section). Different phases (indium, GaAs, InAs, and InGaAs) were identified in the structures. For instance,

Table 1. Experimental conditions.

Parameter	Value
Base pressure (Torr)	1.0×10^{-6}
Work pressure (Torr)	1.0×10^{-3}
Distance target-substrate (cm)	5.0
Deposit temperature of the GaAs layer ($^{\circ}\text{C}$)	580
Deposit temperature of the indium layer ($^{\circ}\text{C}$)	300

indium diffused in the GaAs lattice by substituting gallium at different concentrations across the structure, as schematized in Fig. 1b. This is likely due to a greater mobility of indium atoms at the time of sample preparation. In the first cycle of sample preparation, less distributed indium atoms, led to the formation of an InGaAs ternary semiconductor. However, near the surface, where the concentration of indium was higher, the formation of InAs clusters was more likely.

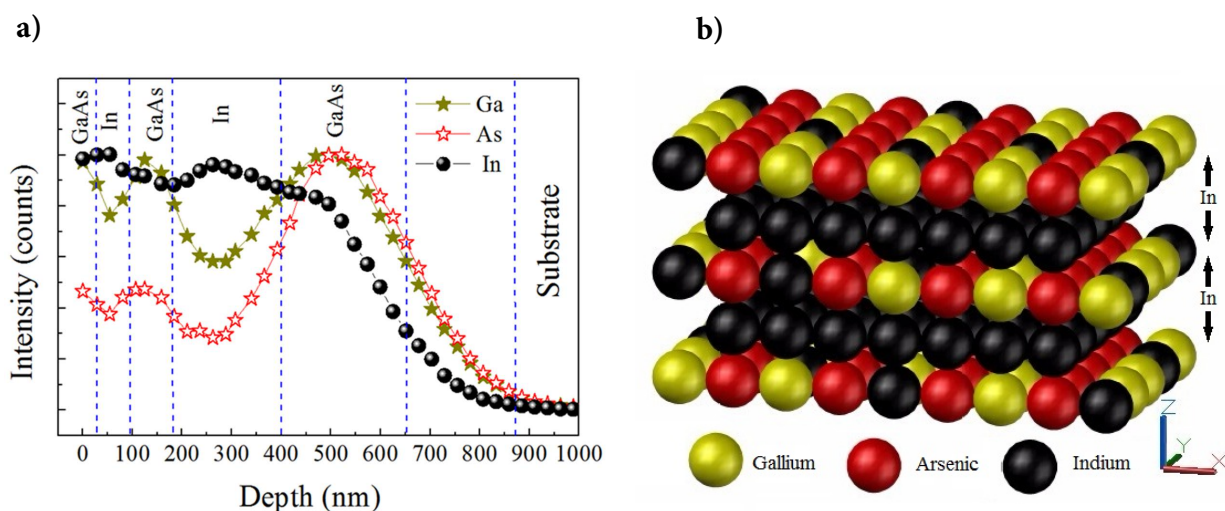


Figure 1. a) SIMS spectrum as a function of depth for the M1 interphase. b) Schematic of the diffusion of elements in the M3 interphase.

The nature of the Ga-As and In-As bond formation and the composition of the InGaAs ternary structure is the result of bonding events in the interface at the time of sample preparation. In order to corroborate this combination of phases throughout the structure, different Raman experiments were carried out and their outcomes described later.

X-ray

The X-ray diffraction spectra for samples M1-3, shown in **Fig. 2**, correspond to deposition of indium layers at 5, 10, and 15 minutes at the end of each structure, respectively. For the analysis, the spectra were normalized with respect to the intensity of the substrate plane located at $2\theta \approx 32.2^\circ$. In each of the spectra, the crystallographic planes corresponding to the indium tetragonal phase, coming from the indium intermediate layers were identified on the background. Similarly, in positions $2\theta \approx 27.5^\circ$, 46.6° , 53.8° , and 55.5° planes with crystallographic directions 111, 202, 311, and 222 were observed. In addition, the following InAs crystallographic planes were identified: 111, 202, 311, and 222. These crystallographic planes were located at $2\theta \approx 25^\circ$, 41.6° , 49.3° , and 50.6° , respectively. Finally, a signal of low intensity was identified between the peaks associated with InAs and GaAs binary semiconductors, possibly due to an InGaAs ternary formation by interfacial diffusion of indium into the GaAs layer.

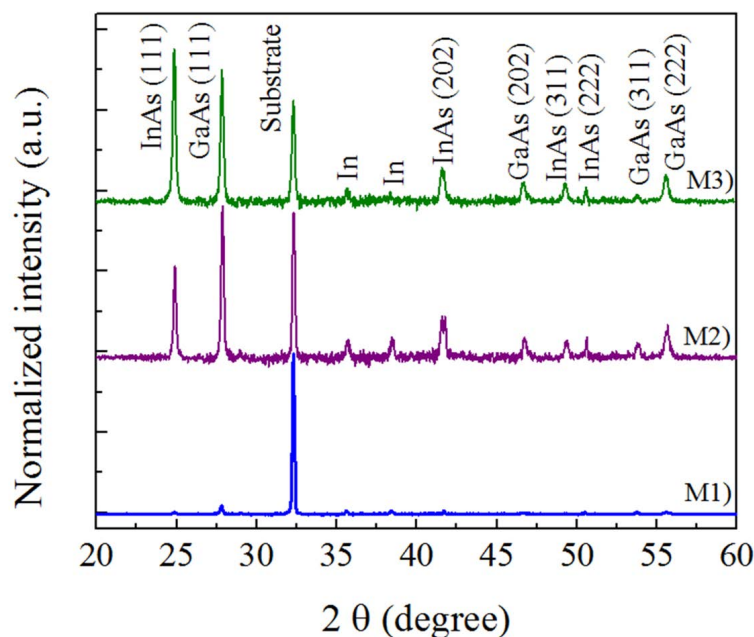


Figure 2. X-ray diffractograms for M1-M3 structures.

As observed in the diffractograms of Fig. 2, the integrated intensities of the $I_{\text{InAs}}/I_{\text{GaAs}}$ ratios increased. These ratios were calculated on the InAs and GaAs plane 111, obtaining values of 0.83, 1.72, and 3.37, across M1 to M3, respectively. These observed ratios revealed an increase of the InAs phase with respect to the GaAs phase due to a surge in the deposition times and/or thickness of the indium intermediate layer. The plane at $2\theta = 32.2^\circ$ corresponds to the Si substrate (100).

Raman

To analyze the influence of the indium intermediate layer on vibrational modes, Raman spectra were taken on the layer's surface and in a cross section along the breadth of the structure. The Raman spectra taken on the layer's surface with laser excitation lines of 452 nm, 532 nm, and 652 nm are indicated in Fig. 3 and Fig. 4. Raman spectra revealed the following: a) A change in the Raman line shape due to an increase in the penetration depth of each laser line; b) A two-mode behavior, typical of III-V alloys, i.e. independent TO and LO phononic modes associated with GaAs and InAs [34-36]. c) All the spectra show a shift of approximately 5 cm^{-1} towards low frequencies with respect to the vibrational modes of GaAs and InAs in bulk, due to the stresses generated in the interfaces during the preparation of the layers. d) A change in integrated intensities and in the width at half of its maximum value (FWHM: full width at half maximum) in InAs and GaAs vibrational modes. These are attributed to a change in the percentage of indium incorporated in GaAs, for interfacial diffusion purposes. Additionally, an LA(L) mode is evidenced in approximately 195 cm^{-1} , possibly due to a structural disorder. Vibrational modes below 200 cm^{-1} correspond to the activation of the longitudinal acoustic mode (disorder activated longitudinal acoustic-DALA), this being the most evident for longer indium deposition times, indicating a greater structural disorder.

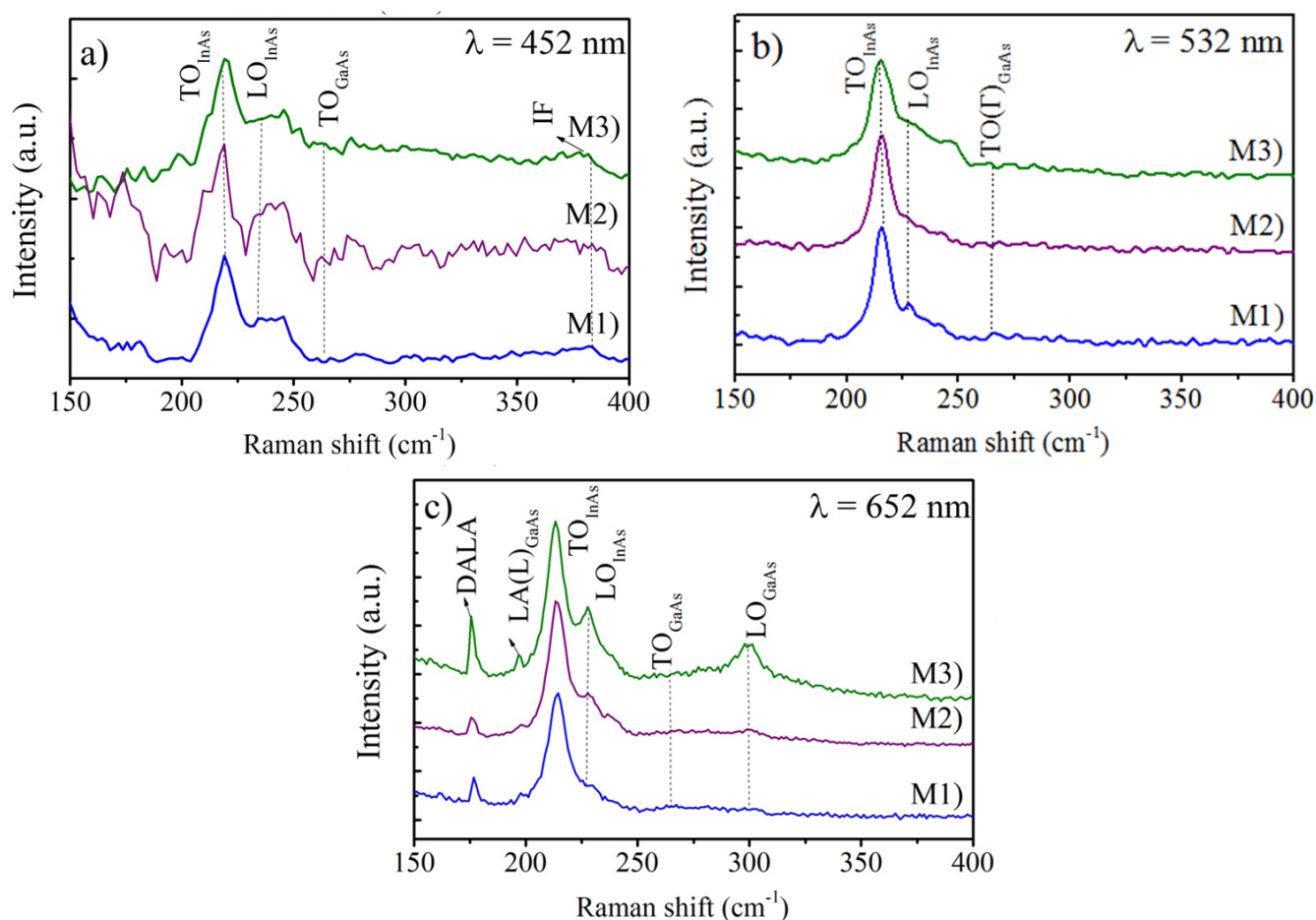
In order to make a more detailed analysis of the Raman spectra taken with different excitation lengths, the penetration depth (δ) of each laser line was calculated using the formula $\delta = \lambda/4\pi k$, where k (extinction coefficient) corresponds to the imaginary part of the complex refractive index $n = n + ik$ [37]. The values obtained, considering indium diffusion in the GaAs layer, are shown in Table 2.

When the M1, M2, and M3 samples were excited with the 452 nm laser (Fig. 3a), the Raman signal comes from a region that is very close to the surface of the sample ($\delta = 81 \text{ nm}$). This is the reason why the spectra are noisy and not very well-defined. However, the vibrational modes of GaAs ($\omega_{\text{TO}} = 263 \text{ cm}^{-1}$) and InAs ($\omega_{\text{TO}} = 218.9 \text{ cm}^{-1}$, $\omega_{\text{LO}} = 219.2 \text{ cm}^{-1}$) were identified. The observed vibrational modes for InAs are caused by the presence of indium in the last

Table 2. Wavelength, excitation energy and penetration length.

λ (nm)	E (eV)	δ (nm)
452	2.54	81
532	2.33	132
652	1.9	251

indium-and-GaAs layers of the nanostructure, resulting in InGaAs formation. The vibrational mode about 400 cm^{-1} , labeled as IF, comes from electronic transitions.

**Figure 3.** Raman spectra of the GaAs/In layers under excitation of a) 452 nm, b) 532 nm, and c) 652 nm.

When the samples are excited with the 532 nm line (Fig. 3b), the Raman signal is more defined because it comes from a depth of $\delta = 132$ nm, and/or a higher volume of Raman excitation ($I_{\text{Raman}} \propto \text{Vol}$). In this case, the TO and LO modes of GaAs and InAs are of greater intensity and have a width at half the maximum, which is lower than in the previous case of the excited sample at 452 nm.

When the samples were excited with lines of a longer wavelength ($\lambda = 652$ nm) and/or penetration $\delta = 252$ nm (Fig. 3c), the Raman signal comes from the proximity of the interface between the second indium and GaAs layer, according to the SIMS concentration profile spectrum. In addition, from the characteristic GaAs phononic modes ($\omega_{\text{LO}} = 300$ cm^{-1}), a vibrational longitudinal acoustic LA mode (Γ) of GaAs ($\omega_{\text{LA}}(\Gamma) = 198$ cm^{-1}) and an acoustic longitudinal mode appeared activated by disorder (DALA) ($\omega_{\text{DALA}} = 175$ cm^{-1}). This is due to the generation of Ga (V_{Ga}) and/or As (V_{As}) vacancies, whose intensity is greater when the deposition time of the In intermediate layer is 15 min.

To analyze the compositional and morphological homogeneity of the indium and GaAs layers, Raman spectroscopy measurements were carried out in a cross section, in areas close to the In and GaAs interface and with the highest probability of GaAs content. The Raman spectra taken with a laser line of $\lambda = 652$ nm at three different depths are shown in Fig. 4. The three depths were: near the surface (Fig. 4a), at 250 nm (Fig. 4b), and 500 nm from the surface (Fig. 4c). These three spectra had similar shapes, but the relative intensities among their phononic modes differed, possibly due to variation of indium concentration within the structure, favoring the formation of Ga-In and/or the InGaAs ternary bonds.

Then, the set of Raman results allows to corroborate indium atoms diffusion in the GaAs layers, as revealed by SIMS and X-ray analyses. Additionally, although the technique for obtaining material used in this work is different from those usually reported, the diffusion kinetics of indium atoms in GaAs can be related to substrate temperature at the time of sample obtention or to the heat exerted on this type of semiconductors [38]. At a characteristic activation temperature or energy, the atoms can have a sufficient mobility favoring surface and volume diffusion. Another factor strongly related to this diffusion mechanism is the minimization of the elastic energy due to atoms reaching the surface and diffusing; implying a variation in the composition [39], which is a consequence of the employed sample obtention method.

Consequently, our results suggest the possibility of obtaining InGaAs/GaAs-type structures through the magnetron sputtering technique using the method previously exposed under controlled experimental conditions. This permits to have control on lattice defects and concentration

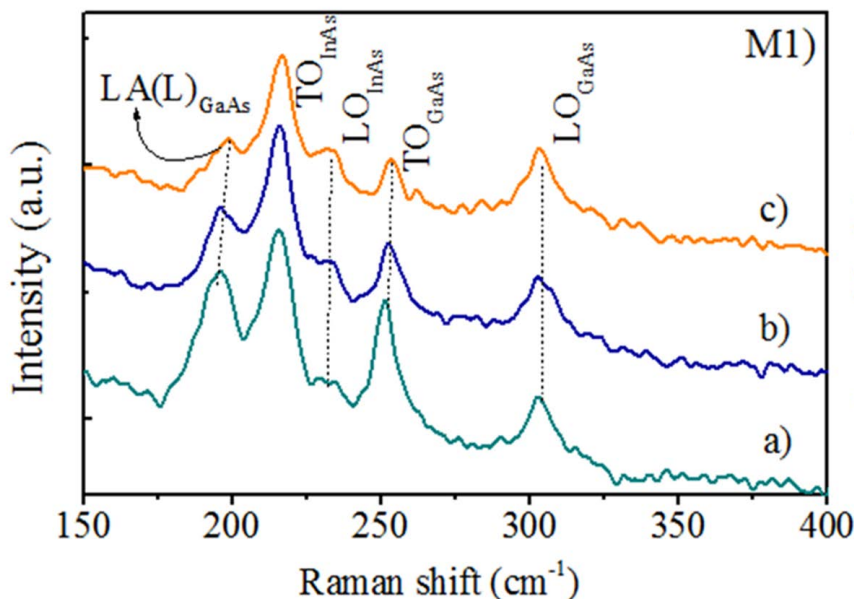


Figure 4. Raman spectra taken in cross section along the structure: a) near the surface, b) at 250 nm, and c) at 500 nm measured from the surface.

gradients among layers. Our approach becomes an alternative among the methods used by magnetron sputtering to control the atoms incorporated in the GaAs lattice.

Conclusions

GaAs/In/GaAs/In/GaAs III-V semiconductor structures were obtained on silicon substrates (100) by a low-cost technique such as magnetron sputtering. The diffusion behavior of the atoms at the interfaces of the alternating GaAs and indium layers was determined from optical, compositional, and structural results. All the samples responded to the diffusion mechanism, which depends on the indium layer deposition time.

Raman analyses led to establishing LO and TO combined vibrational modes, which are characteristic of the substitution of indium atoms by gallium atoms. This corroborates the formation of the InGaAs ternary in some regions of the samples. Alternating semiconductor-metal layers (GaAs/In in this case), resulting in the formation of materials of interest.

Finally, the Magnetron sputtering method can be used for the preparation of semiconductor alloys with different species of metallic elements and

semiconductors, expanding the research spectrum for polycrystalline III-V semiconductor materials.

Acknowledgements

This work was funded with research grants 38416 and 28096 by the Research Department of Universidad Nacional de Colombia, Manizales-DIMA and with the Francisco José de Caldas Scholarship (No. 528) awarded by Colciencias to R. Bernal-Correa. The authors acknowledge the Physics Department at the Centre for Research and Advanced Studies (CINVESTAV) for logistical support.

Conflict of interest

The authors declare having no conflict of interest

References

- [1] Tatavartia SR, Bittner ZS, Wibowo A, Slocum MA, Nelson G, Kum H, Ahrenkiel SP, Hubbard SM. Epitaxial Lift-off (ELO) of InGaP/GaAs/InGaAs solar cells with quantum dots in GaAs middle sub-cell, *Solar Energy Materials and Solar Cells*, 185: 153-157, 2018.
doi: [10.1016/j.solmat.2018.05.016](https://doi.org/10.1016/j.solmat.2018.05.016)
- [2] Bruzzi M, Baldi A, Ennio, Carnevale A, Catelani M, Ciani L. Conversion efficiency of Si-InGaAs and GaAsP-Si-Ge lateral beam splitting photovoltaic devices, *Measurement*, 119: 102-107, 2018.
doi: [10.1016/j.measurement.2018.01.035](https://doi.org/10.1016/j.measurement.2018.01.035)
- [3] Bimberg D. Semiconductor nanostructures for flying q-bits and green photonics, *Nanophotonics*, 7: 1245-1257, 2018.
doi: [10.1515/nanoph-2018-0021](https://doi.org/10.1515/nanoph-2018-0021)
- [4] Ali LM, Abed FA. Investigation the absorption efficiency of GaAs/InGaAs nanowire solar Cells, *Optical Materials*, 72: 650-653, 2017.
doi: [10.1016/j.optmat.2017.07.014](https://doi.org/10.1016/j.optmat.2017.07.014)

- [5] Tex DM, Nakamura T, Imaizumi M, Ohshima T, Kanemitsu Y. Direct evaluation of influence of electron damage on the subcell performance in triple-junction solar cells using photoluminescence decays, *Scientific Reports*, 7: 1-8 2017.
doi: [10.1038/s41598-017-02141-0](https://doi.org/10.1038/s41598-017-02141-0)
- [6] Sayaria A, Ezzidini M, Azeza B, Rekaya S, Shalaan E, Yaghmoura SJ, Al-Ghamdic A, Sfaxid L, Mghaieth R, Maaref H. Improvement of performance of GaAs solar cells by inserting self-organized InAs/InGaAs quantum dot superlattices, *Solar Energy Materials and Solar Cells*, 113: .1-6, 2013.
doi: [10.1016/j.solmat.2013.01.033](https://doi.org/10.1016/j.solmat.2013.01.033)
- [7] Yu P, Wu J, Gao L, Liu H, Wang Z. InGaAs and GaAs quantum dot solar cells grown by droplet epitaxy, *Solar Energy Materials and Solar Cells*, 161: 377-381, 2017.
doi: [10.1016/j.solmat.2016.12.024](https://doi.org/10.1016/j.solmat.2016.12.024)
- [8] Golovynskyi S, Datsenko O I, Seravalli L, Trevisi G, Frigeri P, Babichuk IS, Golovynska I, Qu J. Interband photoconductivity of metamorphic InAs/InGaAs quantum dots in the 1.3-1.55 μm window, *Nanoscale Research Letters*, 13: 103, 2018.
doi: [10.1186/s11671-018-2524-3](https://doi.org/10.1186/s11671-018-2524-3)
- [9] Habchi M, Tounsi N, Bedoui M, Zaied I, Rebey A, El Jani B. Structural and optical properties of $\text{In}_x\text{Ga}_{1-x}\text{As}$ strained layers grown on GaAs substrates by MOVPE, *Physica E: Low-dimensional Systems and Nanostructures*, 56: 74-78, 2014.
doi: [10.1016/j.physe.2013.08.017](https://doi.org/10.1016/j.physe.2013.08.017)
- [10] Essig S, Allebé C, Remo T, Geisz JF, Steiner MA, Horowitz K, Barraud L, Ward JS, Schnabel M, Descoedres A, Young DL, Woodhouse M, Despeisse M, Ballif C, Tamboli A. Raising the one-sun conversion efficiency of III-V/Si solar cells to 32.8 % for two junctions and 35.9 % for three junctions, *Nature Energy*, 2: 1-9, 2017.
doi: [10.1038/nenergy.2017.144](https://doi.org/10.1038/nenergy.2017.144)
- [11] Richter A, Benick J, Feldmann F, Fell A, Hermle M, Glunz SW. n-Type Si solar cells with passivating electron contact: identifying sources forefficiency limitations by wafer thickness and resistivity variation, *Solar Energy Materials and Solar Cells*, 173: 96-105, 2017.
doi: [10.1016/j.solmat.2017.05.042](https://doi.org/10.1016/j.solmat.2017.05.042)

- [12] Green MA, Hishikawa Y, Dunlop E, Levi DH, Ebinger JH, Yoshita M, Ho-Baillie A. Solar cell efficiency tables (version 53), *Progress in Photovoltaics: Research and Applications*, 27: 3-13, 2018.
doi: [10.1002/pip.3102](https://doi.org/10.1002/pip.3102)
- [13] Lassise MB, Wang P, Tracy BD, Chen G, Smith DJ, Zhang YH. Growth of II-VI/III-V heterovalent quantum structures, *Journal of Vacuum Science & Technology B*, 36: 02D110 1-5, 2018.
doi: [10.1116/1.5017972](https://doi.org/10.1116/1.5017972)
- [14] Bakali E, Selamat Y, Tarhan E. Effect of Annealing on the Density of Defects in Epitaxial CdTe (211)/GaAs, *Journal of Electronic Materials*, 47(8): 4780-4792, 2018
doi: [10.1007/s11664-018-6352-0](https://doi.org/10.1007/s11664-018-6352-0)
- [15] Zhang Z, Shen Y, Xu Y, Huang J, Cao M, Gu F, Wang L. Preparation and surface defect regulation of CdZnTe films based on GaN substrates, *Vacuum*, 152: 145-149, 2018.
doi: [10.1016/j.vacuum.2018.03.017](https://doi.org/10.1016/j.vacuum.2018.03.017)
- [16] Kawakita S, Imaizumi M, Makita K, Nishinaga J, Sugaya T, Shibata H, Sato, SI, Ohshima, T. High efficiency and radiation resistant InGaP/GaAs//CIGS stacked solar cells for space applications, *Conference Record of the IEEE Photovoltaic Specialists Conference*, 43: 2574-2577, 2017.
doi: [10.1109/PVSC.2017.8366599](https://doi.org/10.1109/PVSC.2017.8366599)
- [17] Brajesh S, Yadav P, Mohanta P, Srinivasa R, Major S. Electrical and optical properties of transparent conducting $\text{In}_x\text{Ga}_{1-x}\text{N}$ alloy films deposited by reactive co-sputtering of GaAs and indium, *Thin Solid Films*, 555: 179-184, 2014.
doi: [10.1016/j.tsf.2013.11.117](https://doi.org/10.1016/j.tsf.2013.11.117)
- [18] Galiana B, Silvestre S, Algora C, Rey-Stolle I. Effect of annealing atmosphere in the properties of GaAs layers deposited by sputtering techniques on Si substrates, *Journal of Materials Science-Materials in Electronics*, 25: 134-139, 2014.
doi: [10.1007/s10854-013-1562-y](https://doi.org/10.1007/s10854-013-1562-y)
- [19] Chen R, Deng S, Liu Y, Liu Y, Li B, Wong M, Kwok HS. Investigation of top gate GaN thin-film transistor fabricated by DC magnetron sputtering, *Journal of Vacuum Science & Technology B*, 36: 032203 1-5, 2018.
doi: [10.1116/1.5021705](https://doi.org/10.1116/1.5021705)

- [20] Howlader M, Zhang F, Deen M. Formation of gallium arsenide nanostructures in Pyrex glass, *Nanotechnology*, 24: 315301, 2013.
doi: [10.1088/0957-4484/24/31/315301](https://doi.org/10.1088/0957-4484/24/31/315301)
- [21] Bernal-Correa R, Gallardo-Hernández S, Cardona-Bedoya J, Pulzara-Mora A. Structural and optical characterization of GaAs and InGaAs thin films deposited by RF magnetron sputtering, *Optik*, 145: 608-616, 2017
doi: [10.1016/j.ijleo.2017.08.042](https://doi.org/10.1016/j.ijleo.2017.08.042)
- [22] Erlacher A, Ambrico M, Capozzi V, Augelli V, Jaeger H, Ullrich B. X-ray absorption and photocurrent properties of thin-film GaAs on glass formed by pulsed-laser deposition, *Semiconductor Science and Technology*, 19: 1322-1324, 2004.
doi: [10.1088/0268-1242/19/11/019](https://doi.org/10.1088/0268-1242/19/11/019)
- [23] Venegas M, Bernal R, López M, Pulzara A. Microstructure AFM study and raman spectra of In-GaAs bilayers prepared by R.F. magnetron sputtering on Si(100) substrates, *Journal of Physics: Conference Series*, 480: pp. 012017. 2014.
doi: [10.1088/1742-6596/480/1/012017](https://doi.org/10.1088/1742-6596/480/1/012017)
- [24] Aslan M, Yalcın B, Üstündag M. Structural and electronic properties of $\text{Ga}_{1-x}\text{In}_x\text{As}_{1-y}\text{N}_y$ quaternary semiconductor alloy on GaAs substrate, *Journal of Alloys and Compounds*, 519: 55-59, 2012.
doi: [10.1016/j.jallcom.2011.12.020](https://doi.org/10.1016/j.jallcom.2011.12.020)
- [25] Othman M, Kasap E, Korozlu N. Ab-initio investigation of structural, electronic and optical properties of $\text{In}_x\text{Ga}_{1-x}\text{As}$, $\text{GaAs}_{1-y}\text{P}_y$ ternary and $\text{In}_x\text{Ga}_{1-x}\text{As}_{1-y}\text{P}_y$ quaternary semiconductor alloys, *Journal of Alloys and Compounds*, 496: 226-233, 2010.
doi: [10.1016/j.jallcom.2009.12.109](https://doi.org/10.1016/j.jallcom.2009.12.109)
- [26] Zhao J, Shen W, Chang B, Zhang Y, Zhang J, Qin C. Comparison of module structure of wideband response GaAs photocathode grown by MBE and MOCVD, *Optics Communications*, 328: 129-134, 2014.
doi: [10.1016/j.optcom.2014.04.071](https://doi.org/10.1016/j.optcom.2014.04.071)
- [27] Kim Y, Kim K, Wan T, Mawst L, Kuech T, Kim C, Park W, Lee J. InGaAsNSb/Ge double-junction solar cells grown by metalorganic chemical vapor deposition, *Solar Energy*, 102: 126-130, 2014.
doi: [10.1016/j.solener.2014.01.019](https://doi.org/10.1016/j.solener.2014.01.019)

- [28] Fujikura H, Muranaka T, Hasegawa H. Formation of device-oriented InGaAs coupled quantum structures by selective MBE growth on patterned InP substrates, *Physica E: Low-dimensional Systems and Nanostructures*, 7: 864-869, 2000.
doi: [10.1016/S1386-9477\(00\)00078-3](https://doi.org/10.1016/S1386-9477(00)00078-3)
- [29] Ji L, Lu S, Wu Y, Dai P, Bian L, Arimochi L, Watanabe T, Asaka N, Uemura M, Tackeuchi A, Uchida S, Yang H. Carrier recombination dynamics of MBE grown InGaAsP layers with 1 eV bandgap for quadruple-junction solar cells, *Solar Energy Materials and Solar Cells*, 127: 1-5. 2014.
doi: [10.1016/j.solmat.2014.03.051](https://doi.org/10.1016/j.solmat.2014.03.051)
- [30] Yanping Y, Chunling L, Zhongliang Q, Mei L, Xin G, Baoxue B. Optical and Electrical Properties of a-InGaAs:H Films Prepared by Double-Target Magnetron Co-sputtering, *IEEE International Nanoelectronics Conference*, 2: 411-414, 2008.
doi: [10.1109/INEC.2008.4585516](https://doi.org/10.1109/INEC.2008.4585516)
- [31] Bernal-Correa R, Gallardo-Hernández S, Cardona-Bedoya J, Pulzara-Mora A, Structural and optical characterization of GaAs and InGaAs thin films deposited by RF magnetron sputtering, *Optik*, 145: 608-616, 2017.
doi: [10.1016/j.ijleo.2017.08.042](https://doi.org/10.1016/j.ijleo.2017.08.042)
- [32] Van Der Heider P, Secondary Ion Mass Spectrometry: An Introduction to Principles and Practices, *Wiley New Jersey, Estados Unidos*. 2014.
doi: [10.1002/9781118916780](https://doi.org/10.1002/9781118916780)
- [33] Dhaval A, Sharma SK, Sharma RK, Kapoor AK. Characterisation of Semiconductor Materials/Device Structures using SIMS, *Defence Science Journal*, 59: 342-350, 2009.
doi: [10.14429/dsj.59.1532](https://doi.org/10.14429/dsj.59.1532)
- [34] Groenen J, Carles R, Landa G, Guerret C, Fontaine C, Gendry M. Optical-phonon behavior in Ga_{1-x}In_xAs: The role of microscopic strains and ionic plasmon coupling, *Physical Review B*, 58: 452-462, 1998.
doi: [10.1103/PhysRevB.58.10452](https://doi.org/10.1103/PhysRevB.58.10452)

- [35] Sim E, Han M, Beckers J, leeuw S. Local structure invariant potential for $\text{In}_x\text{Ga}_{1-x}\text{As}$ semiconductor alloys, *Bulletin of Korean Chemical Society*, 30: 857-862, 2009.
doi: [10.5012/bkcs.2009.30.4.857](https://doi.org/10.5012/bkcs.2009.30.4.857)
- [36] Islam MR, Verma P, Yamada M, Kodama S, Hanauer Y, Kinoshita K. The influence of residual strain on Raman scattering in $\text{In}_x\text{Ga}_{1-x}\text{As}$ single Crystals, *Materials Science and Engineering*, 91: 66-69, 2002.
doi: [10.1016/S0921-5107\(01\)00972-2](https://doi.org/10.1016/S0921-5107(01)00972-2)
- [37] Feng ZC, Allerman A, Barnes PA, Perkowitz S. Raman scattering of InGaAs/InP grown by uniform radial flow epitaxy, *Applied Physics Letters*, 60: 1848, 1992.
doi: [10.1063/1.107187](https://doi.org/10.1063/1.107187)
- [38] Kawai T, Yonezu H, Ogasawara Y, Saito D, Pak K. Segregation and interdiffusion of in atoms in GaAs/InAs/GaAs heterostructures, *Journal Applied Physics*, 74: 1770-1774, 1993.
doi: [10.1063/1.354806](https://doi.org/10.1063/1.354806)
- [39] Roura P, Vila A, Bosch J, López M, Cornet A, Morante JR, Westwood DI. Atomic diffusion induced by stress relaxation in InGaAs/GaAs epitaxial layers, *Journal Applied Physics*, 82: 1147-1152, 1997.
doi: [10.1063/1.365881](https://doi.org/10.1063/1.365881)

Estudio estructural y óptico de nanoestructuras de arseniuro de indio y galio preparadas por pulverización catódica por magnetrón

Resumen: Actualmente, la obtención de nanoestructuras basadas en materiales tipo III-V es costosa. Para ello se requieren enfoques de fabricación de nanoestructuras novedosos y económicos. En este trabajo, presentamos resultados sobre la fabricación de nanoestructuras que consisten en capas alternas de In y GaAs en un sustrato de Si mediante pulverización catódica con magnetrón. Además, caracterizamos las nanoestructuras producidas utilizando espectroscopía de masas de iones secundarios (SIMS), análisis de difracción de rayos X y espectroscopía Raman. La SIMS reveló variación en la concentración de átomos de In en las interfases de In/GaAs/In, y la difracción de rayos X reveló planos correspondientes a fases asociadas con GaAs e InAs debido a la difusión interfacial de a través de capas de GaAs. Finalmente, para estudiar la composición y la calidad de los cristales de las nanoestructuras fabricadas, se tomaron espectros Raman utilizando líneas de excitación láser de 452 nm, 532 nm y 562 nm en diferentes puntos de las nanoestructuras. Esto permitió determinar los modos ópticos transversales y longitudinales de GaAs y InAs, característicos de un comportamiento de dos modos. Se observó un modo vibratorio longitudinal acústico $LA(\Gamma)$ de GaAs y un modo longitudinal acústico activado por desorden (DALA). Estos modos resultaron de la sustitución de átomos de Ga por átomos de In en altas concentraciones debido a la generación de vacantes de Ga (VGa) y/o As (VA). Estos análisis muestran que la pulverización catódica por magnetrón puede ser una técnica viable y de costo relativamente bajo para obtener este tipo de semiconductores.

Palabras clave: semiconductores tipo III-V; espectroscopía Raman; SIMS; rayos X.

Estudo estrutural e óptico de nanoestruturas de índio e arseneto de gálio, preparadas por pulverização catódica por magnetron

Resumo: Atualmente, a obtenção de nanoestruturas baseadas em materiais do tipo III-V é cara. Isso exige abordagens de fabricação de nanoestruturas inovadoras e econômicas. Neste trabalho, apresentamos resultados sobre fabricação de nanoestruturas que consistem em camadas alternadas de In e GaAs em um substrato de Si por pulverização por magnetron. Além disso, caracterizamos as nanoestruturas produzidas usando espectroscopia de massa de íons secundários (SIMS), análise de difração de raios-X e espectroscopia Raman. O SIMS revelou variação na concentração de átomos de In nas interfaces In/GaAs/In e a difração de raios X revelou planos correspondentes a fases associadas a GaAs e InAs devido à difusão interfacial de In através de camadas de GaAs. Finalmente, a fim de estudar a composição e a qualidade dos cristais das nanoestruturas fabricadas, os espectros Raman foram obtidos usando linhas de excitação a laser de 452 nm, 532 nm e 562 nm em diferentes pontos das nanoestruturas. Isso permitiu determinar os modos ópticos transversal e longitudinal de GaAs e InAs, característicos de um comportamento de dois modos. Foram observados um modo vibracional longitudinal acústico LA(Γ) de GaAs e um modo longitudinal acústico ativado por distúrbio (DALA). Esses modos resultaram da substituição de átomos de Ga por átomos de In em altas concentrações devido à geração de vagas de Ga (VGa) e/ou As (VAs). Essas análises mostram que a pulverização catódica por magnetron pode ser uma técnica viável e de custo relativamente baixo para obter este tipo de semicondutores.

Palavras-chave: semicondutores tipo III-V; espectroscopia Raman; SIMS; raios-X.

Santiago Torres-Jaramillo

Is a Physics Engineer and M.Sc. in Physics graduated from National University of Colombia, he has worked in research area around five years on topics, such as: obtaining III-V materials by Magnetron Sputtering, characterization technics, and theoretical calculations of tandem solar cells based on CIGS and III-V materials coupled with silicon.

ORCID: [0000-0001-9652-3225](https://orcid.org/0000-0001-9652-3225)

Camilo Pulzara Mora

Is a physics engineer earning his bachelor's degree at Universidad Nacional de Colombia at Manizales, Colombia. Currently, he is enrolled in a MSc Physics and his research is focused on III-V semiconductors doped with transition metals, such as Mn, deposited by r.f magnetron sputtering. Structural, magnetic and electrical characterizations have been made to study and to try to synthesize diluted magnetic semiconductors using a low-cost technique.

ORCID: [0000-0001-9652-3225](https://orcid.org/0000-0001-9652-3225)

Roberto Bernal Correa

Roberto Bernal Correa is an Assistant Professor at the Universidad Nacional de Colombia, Orinoquía headquarters. He is a Physics Engineer from the Universidad Nacional de Colombia and received the M.Sc. Physics and PhD in engineering degrees at the same University. Currently, he carries out research related to the obtaining and characterization of semiconductor materials, and the theoretical design of solar cells.

ORCID: [0000-0001-9339-6574](https://orcid.org/0000-0001-9339-6574)

Salvador Gallardo Hernandez

He completed his MSc and PhD at the Electrical Engineering Department of Cinvestav. He did his first post-doctoral training at Applied Physics Department of the Physics Institute, Sao Paulo University, Brazil, in the laboratory of Dr. Sergio Morelhao and two sort stances at LNLS (Laboratório Nacional de Luz Síncrotron); he developed a deep interest for crystallography. Dr. Gallardo-Hernandez is nowadays Professor at the Nanoscience and Nanotech Program and at Physics Department of Cinvestav.

ORCID: [0000-0001-6968-5560](https://orcid.org/0000-0001-6968-5560)

Miguel Venegas de la Cerda

Miguel A. Venegas, Staff-R&D Scientist at RHK Technology, worked on Cryogenic Closed Cycles SPM, FM-AFM and Qplus technology. During his postdoctoral research in the Solid State and SC Nanostructures groups, Physics Department CINVESTAV-IPN got focused on SC heterostructures characterization. On organic molecules on ultra-thin insulating films on Au(111) in the Nanotechnology and Molecular Engineering Laboratory, UAM-I. He earned his Ph.D. in Nanosciences in the Group of Nanoscience (CEMES-CNRS) Toulouse, France.

ORCID: [0000-0001-9797-4431](https://orcid.org/0000-0001-9797-4431)

Álvaro Pulzara Mora

Alvaro Pulzara Mora is a Teacher - Researcher at the National University of Colombia, Manizales campus. PhD. Sciences - Physics. Graduated from (CINVESTAV), of the National Polytechnic Institute, Mexico City. Master of Science - Physics. Universidad del Valle, Cali - Colombia. Investigating in semi-conductors III-V and (III-V) (M, Cr) semi-magnetic grown by magnetron sputtering on substrates in different orientations (nn1), for applications in solar cells and optoelectronic devices.

ORCID: [0000-0003-1648-1788](https://orcid.org/0000-0003-1648-1788)

Máximo López López

Dr. López López studied the degree in Physics and Mathematics at the ESFM-IPN. He obtained his Master of Science degrees with a specialty in Physics from CINVESTAV-IPN and PhD from the Toyohashi University of Technology, Japan. His lines of research include Synthesis of Semiconductor Nanostructures, semiconductor film growth by molecular beam epitaxy (MBE), the fabrication and characterization of low dimensional structures: Wells, Wires and Quantum Dots.

ORCID: [0000-0002-46476683](https://orcid.org/0000-0002-46476683)